

Structural studies of bismuth nanocrystals embedded in SiO₂ or GeO₂ matrices

B. Kusz^{a)}

Faculty of Applied Physics and Mathematics, Gdańsk University of Technology, Narutowicza 11/12, 80-952 Gdańsk, Poland

D. Pliszka

Institute of Physics, Pomeranian Pedagogical Academy, Arciszewskiego 22B, 76-200 Słupsk, Poland

M. Gazda

Faculty of Applied Physics and Mathematics, Gdańsk University of Technology, Narutowicza 11/12, 80-952 Gdańsk, Poland

R. S. Brusa

INFN, Dipartimento di Fisica, Università di Trento, 38-050 Povo, Italy

K. Trzebiatowski

Faculty of Applied Physics and Mathematics, Gdańsk University of Technology, Narutowicza 11/12, 80-952 Gdańsk, Poland

G. P. Karwasz and A. Zecca

INFN, Dipartimento di Fisica, Università di Trento, 38-050 Povo, Italy

L. Murawski

Faculty of Applied Physics and Mathematics, Gdańsk University of Technology, Narutowicza 11/12, 80-952 Gdańsk, Poland

(Received 15 April 2003; accepted 18 September 2003)

The layer of bismuth nanoclusters embedded in glass matrices and the surface layer of bismuth grains have been obtained by thermal treatment in hydrogen atmosphere of Bi_{0.33}Ge_{0.67}O_{1.84} and Bi_{0.57}Si_{0.43}O_{1.72} glass. The thickness and structure of such layers strongly depend on temperature and time of reduction. The structural studies of bismuth nanocrystals embedded in SiO₂ or GeO₂ matrices were performed with optical microscopy and atomic force microscopy. By the use of a slow-positron beam we monitored the structural changes undergoing in near-to-surface layers after the first steps of isothermal annealing. A simple two-layer model of reduced glasses explains the evolution of the surface layer and electrical properties of the material during the reduction process.

© 2003 American Institute of Physics. [DOI: 10.1063/1.1624484]

I. INTRODUCTION

Bismuth silicate glasses are interesting materials, which find many special applications.^{1,2} Bismuth germanate and bismuth silicate glasses, in the course of heat treatment in hydrogen atmosphere, change their physical properties. For instance, the surface conductivity increases by several orders of magnitude during an appropriate heat treatment. Changes of material properties are directly related to the evolution of the structure and morphology of the glass surface. Annealing in hydrogen reduces Bi³⁺ ions into neutral atoms, which subsequently agglomerate into granules on the surface and inside the glass. The properties of reduced bismuth–silicate glasses have been investigated^{3–5} but only a few works have been published on the physical properties of nonreduced⁶ and reduced^{7,8} bismuth germanate glasses and there still remain many questions about the conductivity and structure of these materials.

In this article, we present experimental studies of Bi nanocrystals embedded in SiO₂ and GeO₂ matrices. A two-

layer model of the reduced glasses is discussed. We also analyze the possible influence of the diffusion of bismuth towards the surface on the stoichiometry of reduced glasses.

II. EXPERIMENT

Glasses of nominal composition Bi_{0.33}Ge_{0.67}O_{1.84} and Bi_{0.57}Si_{0.43}O_{1.72} were synthesized as follows. A milled mixture of powdered SiO₂ or GeO₂ and bismuth nitrate, placed into a platinum crucible, was decomposed at 1000 K for 1 h. After that, the mixture was ground again and submitted to a gradual heating from room temperature to 1500 K. Melted material was homogenized by mechanical stirring and then quenched by pouring onto a steel plate. Before further treatment the surface of samples were polished and cleaned carefully. The nominal oxygen content in the glass was calculated within the assumption that the original glass has a composition determined by the valency 3⁺ of Bi and 4⁺ of Ge and Si.

The reduction process was carried out at 613 K in hydrogen atmosphere. In this article, we present results obtained for Bi_{0.33}Ge_{0.67}O_{1.84} samples reduced for 0.8 h (G1), 2

^{a)}Electronic mail: bodzio@mif.pg.gda.pl

h (G2), 4 h (G2a), 7 h (G3), 12 h (G4), 24 h (G5), and 44 h (G6). In the case of $\text{Bi}_{0.57}\text{Si}_{0.43}\text{O}_{1.72}$ glass, samples reduced for 0.3 h (S1a), 0.5 h (S1b), 0.8 h (S1c), 2 h (S2), 5 h (S3), 24 h (S4), and 44 h (S5) were studied. With aim to calculate the total mass of reduced bismuth and the amount of Bi, which creates the outer layer, the material was weighted before and after the reduction. Cross sections of reduced samples were tested by scanning electron microscopy and by optical microscopy.

Measurements of the conductivity were made using two- or four-terminal methods. The surface conductivity of the samples has been calculated from equation: $\sigma_{\square} = R^{-1}d/l$, where R is the resistance of sample, d the distance between the electrodes, and l their length.

Positron annihilation spectroscopy (PAS) aims to detect structural defects and/or the presence of different phases in materials.⁹ The use of a variable-energy positron beam allows us to study depth-resolved profiles of the material down to a few micrometer-deep layers.¹⁰ A slow positron beam with energy variable between 50 eV and 25 keV was obtained by moderating positrons from a 30 mCi $^{22}\text{NaCl}$ radioactive source in a 1- μm -thick single-crystal tungsten foil. Details about apparatus and the measurement techniques are reported in Ref. 9.

The shape of the 511 keV annihilation line has been characterized by two width parameters. The S parameter was calculated as the ratio of the counts in the central area of the peak $|511.0 - E_{\gamma}| \leq 0.85$ (in keV) and the total area of the peak $|511.0 - E_{\gamma}| \leq 4.25$ (in keV). The S parameter indicates how many positrons annihilate with low-momentum (valence) electrons. Its exact value depends somewhat on the energy resolution of the gamma detection. Therefore, it is usually normalized to the S value in defect-free, high-purity silicon; in our setup the defect-free Si shows a 0.522 value in bulk. Generally, the rise of the S parameter indicates more defects in the material.

The W parameter is defined as “wings” $1.6 \leq |511.0 - E_{\gamma}| \leq 4.0$ (in keV), indicating annihilation with high-momentum (core) electrons. Additionally, the “valley” V parameter indicates the fraction of positrons annihilating in three- γ events, i.e., the low-energy part of the spectrum $E_{\gamma} \leq 501.0$ keV. As three- γ events correspond to annihilation of orthopositronium, the rise of the V parameter indicates the presence of free space (nanovoids) inside the material.

Doppler shape parameters were measured as a function of the positron implantation energy. The implantation depth (in \AA) has been obtained from positron energy using the formula: $d = (400/\rho)E^{1.6}$ with E being the beam energy and ρ the glass density (5.77 and 6.46 g/cm^3 for bismuth-germanate and bismuth-silicate glasses).

III. RESULTS

The reduction process in bismuth-silicate and bismuth-germanate glasses was investigated by isothermal measurements of dc conductivity. The plots of surface conductivity versus reduction time of $\text{Bi}_{0.33}\text{Ge}_{0.67}\text{O}_{1.84}$ and $\text{Bi}_{0.57}\text{Si}_{0.43}\text{O}_{1.72}$ samples reduced at 613 K are presented in Fig. 1. Also, in Fig. 1, the dependence of the thickness of the reduced layer

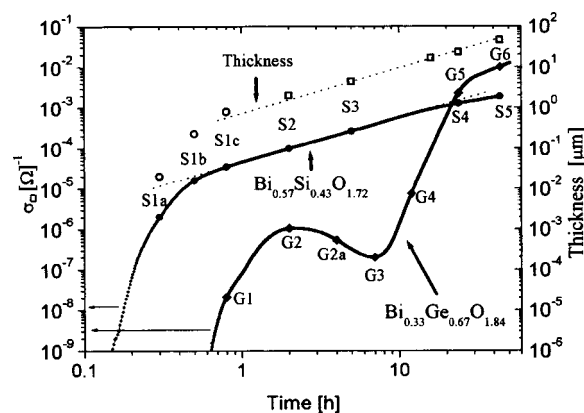


FIG. 1. Time dependence of surface conductivity of $\text{Bi}_{0.33}\text{Ge}_{0.67}\text{O}_{1.84}$ (solid line G1–G6) and $\text{Bi}_{0.57}\text{Si}_{0.43}\text{O}_{1.72}$ (solid line S1a–S5) glasses during heat treatment at 613 K (log–log scale). Empty points and dotted line show the plot of the reduced layer thickness S1a–S5 samples as a function of reduction time. Empty circles are results derived from PAS, empty squares, from optical microscope measurements.

of $\text{Bi}_{0.57}\text{Si}_{0.43}\text{O}_{1.72}$ samples on reduction time is shown. The capital letters marked in Fig. 1 denote the reduction times, which were applied to particular samples taken in further studies. It can be seen that bismuth-germanate and bismuth-silicate glasses exhibit different time dependencies during heat treatment in hydrogen. The curve of $\text{Bi}_{0.33}\text{Ge}_{0.67}\text{O}_{1.84}$ presents the behavior, which is typical of bismuth-germanate glasses.⁸ First, after some time, a rapid, by a few orders of magnitude, increase in the surface conductivity appears. Next, the surface conductivity attains a maximum (about $10^{-6} \Omega^{-1}$) and decreases to a minimum. Further reduction causes an increase of conductivity by a few orders. In contrast to bismuth germanate glass, the conductivity of the $\text{Bi}_{0.57}\text{Si}_{0.43}\text{O}_{1.72}$ sample continuously increases during the reduction.

The layered structure of the reduced samples is visible in atomic force microscope (AFM) and optical microscope images. Figure 2(a) presents AFM pictures chosen for characteristic samples, e.g., G1, G3, and G5. The flat surface of the glass (G1), a layer of connected or disconnected droplets (G3), and multilayer granular systems (G5) are visible on the surface of the samples. The diameters of the granules of bismuth on the surfaces of G3 and G5 are about 30–35 nm. An optical microscope photograph of a cross section of the sample reduced for 44 h at 613 K (G6 and S5) and the surface of the S5 sample are visible in Fig. 2(b). It shows large bismuth spheres (diameter up to about 30 μm) on the surface (S5) and in the reduced layers. The thicknesses of the inner layers are 45 and 4 μm in the S5 and G6 samples, respectively.

The dependences of the S parameter on the positron-beam energy E for as-grown and reduced $\text{Bi}_{0.33}\text{Ge}_{0.67}\text{O}_{1.84}$ and $\text{Bi}_{0.57}\text{Si}_{0.43}\text{O}_{1.72}$ glasses are shown in Figs. 3 and 4, respectively. These dependences give clear information on the layered structures of the samples, using a nondestructive technique.

Identification of the types of sites for positron annihilation are presented in Fig. 5.

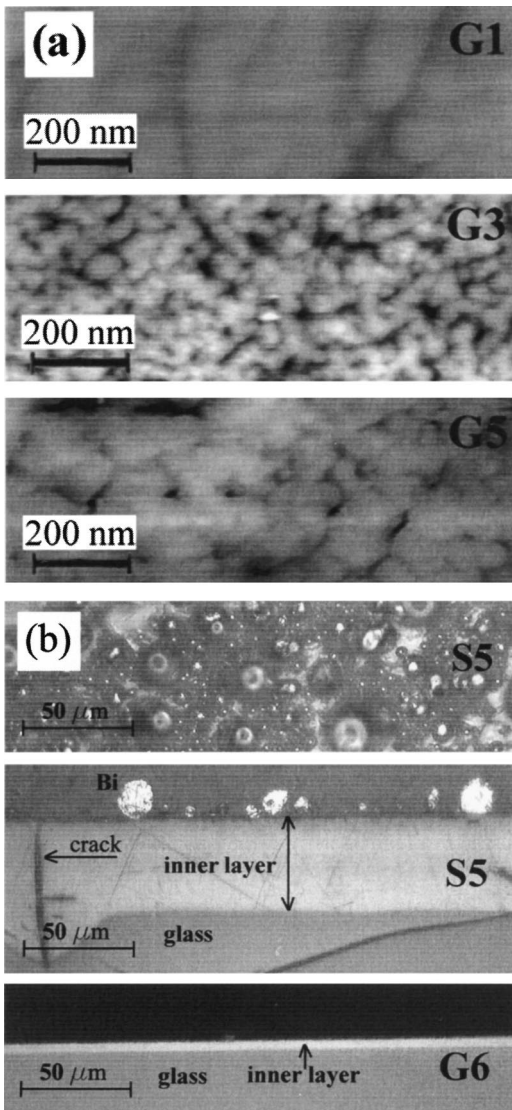


FIG. 2. (a) AFM pictures of $\text{Bi}_{0.33}\text{Ge}_{0.67}\text{O}_{1.84}$ (G1, G3 and G5) samples. (b) Optical microscope photograph of a cross section of the sample reduced for 44 h at 613 K (G6 and S5) and the surface of the S5 sample.

IV. MODEL OF TWO-LAYERED STRUCTURE OF REDUCED IN HYDROGEN GLASS SURFACES

The structural transformations of these glasses heated in hydrogen atmosphere depend both on the time and tempera-

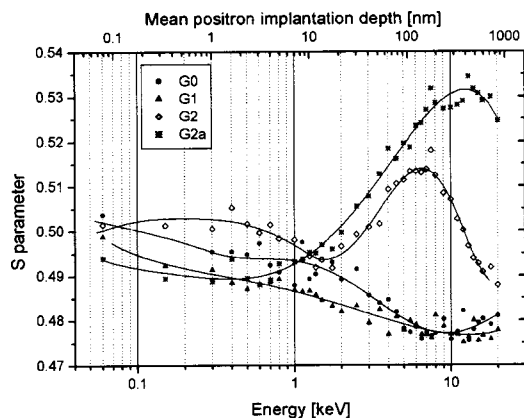


FIG. 3. Doppler broadening S -parameter dependence for $\text{Bi}_{0.33}\text{Ge}_{0.67}\text{O}_{1.84}$ glasses.

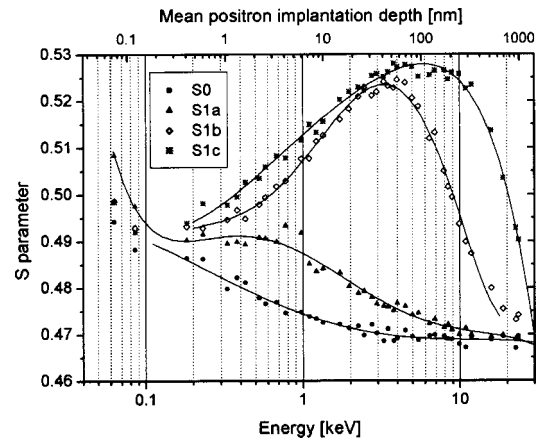


FIG. 4. Doppler broadening S -parameter dependence for $\text{Bi}_{0.57}\text{Si}_{0.43}\text{O}_{1.72}$ glasses.

ture of reduction. It is assumed that during reduction three main phenomena occur in the material: reduction of Bi^{+3} ions into neutral atoms, their agglomeration into bigger clusters, and migration towards the surface of the sample. Taking into account the experimental results of x-ray diffraction (XRD) and atomic force microscopy, we have proposed a simple model of a two-layered structure of the reduced surface.¹¹ The model is illustrated in Fig. 6. In the course of reduction, two conductive layers can be distinguished. The first one is the layer that contains Bi particles embedded in a GeO_2 or SiO_2 glass matrix. The second conducting layer is the very top one containing either a majority of Bi and a small amount of Ge in the case of bismuth–germanate glasses or only Bi in bismuth–silicate glasses.

Within this model we can explain the behavior of the glasses during reduction. As long as the distance between the Bi nanostructures embedded in the glass matrices is too large for electron tunneling to take place, the conductivity is low. While the reduction is carried on, the concentration and dimensions of Bi clusters grow. At a certain time, the Bi concentration on the surface layer of the glasses is sufficient and

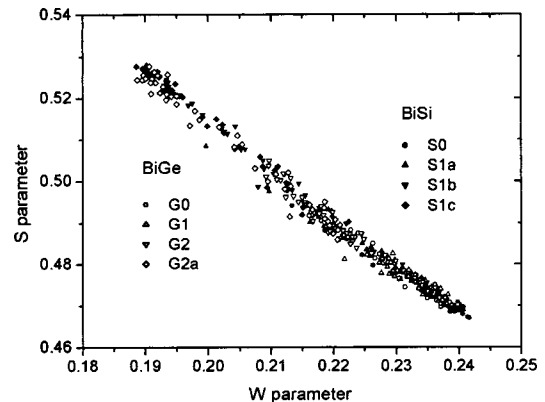


FIG. 5. Identification of types of sites for positron annihilation. Straight-line dependence indicates only two phases, where positrons annihilate. The S parameter was calculated as the ratio of the counts in the central area of the peak $|\Delta E| \leq 0.85$ (in keV) and the total area of the peak $|\Delta E| \leq 4.25$ (in keV). The W parameter is defined as “wings” $1.6 \leq |\Delta E| \leq 4.0$ (in keV).

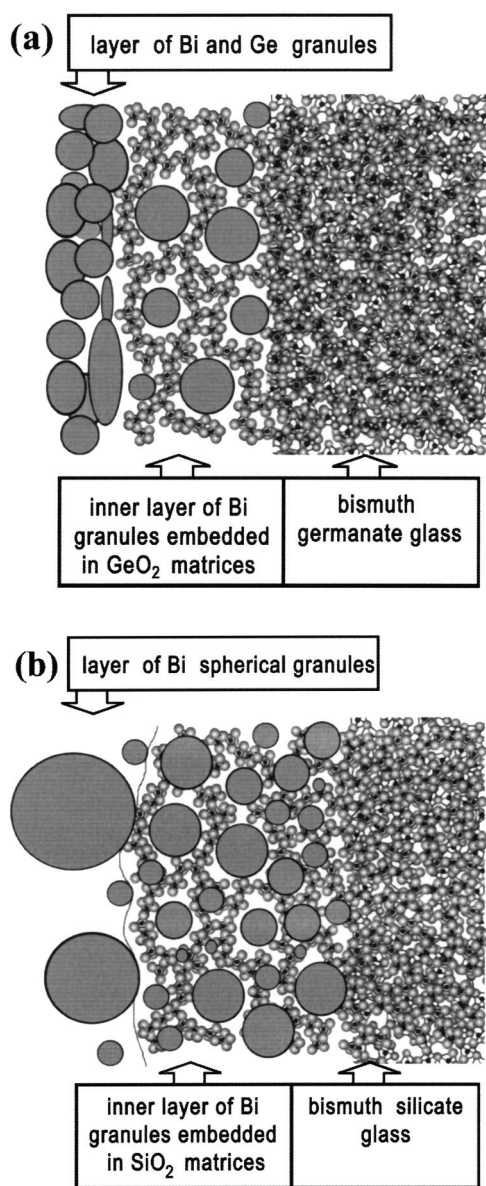


FIG. 6. Model of the layered structure of reduced in hydrogen bismuth-germanate (a) and bismuth-silicate (b) glasses.

electron tunneling through the potential barrier between metallic granules appears. Starting from this moment, the conductivity rapidly increases (Fig. 1, abrupt increase in the conductivity up to point around G1 and S1). In other words, a two-dimensional layer of Bi granules embedded in GeO₂ or SiO₂ matrices is created.

Further reduction causes growing of the layer thickness and the conductivity still increases. In the next stage of reduction process, both the migration of bismuth atoms towards the surface and their agglomeration into large grains become significant. In the case of bismuth-silicate glasses, a layer of nonbonded, spherical bismuth granules on the surface is created, whereas in bismuth-germanate glasses a layer of granules strongly bonded to the surface grows. The difference between both samples is that Ge³⁺ ions are also reduced into neutral atoms while the Si³⁺ ions are not. We believe that this is a reason why the conductivity in bismuth-germanate glasses decreases for some period of

time (between G2 and G3). A further reduction causes a continuous monolayer of Bi granules to be created, and its electrical properties begin to determine the surface conductivity. The thickness of this outer layer increases during longer times of reduction (samples G4, G5, and G6), see our Ref. 8 for more-detailed studies of the structure and the electric conductivity of the outer layer of reduced bismuth-germanate glasses.

V. STOICHIOMETRY AND STRUCTURE OF REDUCED LAYER

During the reduction, a part of neutral Bi atoms migrate towards the surface of the glass. It inevitably changes the stoichiometry of the reduced layer. Apart from this, also, the loss of oxygen, forming cracks and bismuth evaporation, may be considered as possible reasons of changes of the reduced layer composition. With an aim to estimate its real composition, the following measurements were performed:

- measurements of the mass of the oxygen lost were carried out by evaluating the weight loss;
- measurements of the mass of bismuth located in the outer layer (estimated on the basis of the difference between the sample mass before and after removing outer layer);
- comparative measurements of the change in the mass of metallic powdered bismuth (grain dimensions were of the order of tenth micrometers) heated for 44 h in hydrogen atmosphere at temperature 613 K were performed; and
- measurements of the thickness of the reduced layers.

The experimentally measured thicknesses of the reduced layer in the S5 and G6 samples are 45 and 4 μm [Fig. 2(b)], respectively. Taking into account that each neutral bismuth atom (before the reduction process) shares on average 1.5 atoms of oxygen and about 10% of Bi precipitates into cracks, we estimated the thickness and real stoichiometry of the reduced layer of the Bi_{0.53}Si_{0.47}O_{1.72} (S5) and Bi_{0.33}Ge_{0.67}O_{1.84} (G6) samples. If we assume that all the reduced bismuth exists as neutral atoms, the density calculations give the depth of the region where the glasses have been reduced to be equal to 72 and 6.8 μm in the S5 and G6 samples, respectively. The difference between the measured and evaluated thicknesses can be explained by shrinking of the layer connected with lost oxygen, migration of Bi atoms into the surface, creation of cracks, and partial vaporizing of Bi from the surface. Experiment C shows that less than 1% of the mass of granular bismuth evaporated during the 44 h reduction. This value is small but may cause an overestimation of the mass of reduced bismuth (and so, the thickness of the reduced layer).

Summarizing, we think that the reduced layer is a composite of bismuth nanoclusters embedded in a Si(Ge)⁴⁺-2O²⁻ network. Because of the migration of Bi atoms their concentration in the reduced layer decreases. Then, we suppose that the estimated real stoichiometry of the reduced layer is Bi_x-(SiO₂)_{1-x} with 0.41 < x < 0.47. The lower limit was estimated under the assumption that during

the reduction 1% Bi evaporates and 10% Bi precipitates into cracks. The outer layer of the G6 sample is bounded strongly to the glass surface, then it is hard to estimate the real composition of the Bi–GeO₂ layer. Less accurate estimations give Bi_x–(GeO₂)_{1–x} with 0.25 < *x* < 0.3.

Our model of reduced glasses agrees very well with the results of XRD, differential scanning calorimetry (DCS), and AFM analysis.¹¹ The analysis of broadening of XRD peaks shows that the diameter of the embedded Bi nanoparticles in the reduced G6 and S3 samples are about 10 and 8 nm, respectively.

In the case of Bi_{0.53}Si_{0.47}O_{1.72}, a linear increase of conductivity is observed during reduction from 0.8 up to 5 h (see in Fig. 1). Such a phenomenon can be explained assuming that during reduction the structure of the reduced layer does not change and only its thickness grows. It means that the distribution of dimensions of Bi granules embedded in the SiO₂ matrices does not change in the course of reduction. The structure of the reduced layer at 613 K in Bi_{0.57}Si_{0.43}O_{1.72} seems to be stable and does not depend on the reduction time (only its thickness increases). This suggestion is supported by analysis of the melting point of the bismuth nanocrystals embedded in SiO₂ matrices.¹¹ In the samples reduced longer than 5 h the many cracks of the reduced layer are observed. We think that these phenomena cause the change in the slope of the $\sigma_{\square}(t)$ function (Fig. 1, than 5 h many cracks).

VI. POSITRON-ANNIHILATION DEPTH PROFILES

The *S*-parameter measurements indicate a substantial difference between as-received and reduced glasses (see in Figs. 3 and 4). Both nonreduced glasses (G0 and S0) show the *S* parameter in bulk (0.47–0.49) smaller than the values for reduced samples (0.52–0.54 at their maxima). The value of the *S* parameter of the S0 sample (0.47) is somewhat smaller than the literature value for nondefected amorphous SiO₂, which would be 0.50 with our gamma-energy detection resolution.¹² Compared to our previous measurements for lower Bi content silicon glasses Bi_{0.47}Si_{0.53}O_{1.77},¹³ the present bulk *S* parameter is somewhat lower (0.49 for the low Bi content versus about 0.47 in the present samples), reflecting the change in stoichiometry.

The increase of the *S* parameter in the reduced samples compared to the unreduced ones indicates that the reduction process causes the creation of new traps for positrons. During the reduction, H₂ molecules diffuse into glass and neutral Bi atoms and water particles migrate out of the glass. According to our model, the reduced layer is a composite of metallic spheres of bismuth embedded into a well-relaxed (SiO₄)^{4–} or (GeO₄)^{4–} tetrahedral sublattice. In this sublattice and on Bi precipitates/glass interfaces different types of vacancy-like defects exist, raising the probability of positron trapping and successive annihilation with low-momentum electrons.

Positron measurements allow us to trace the depth of the reduced layer, at the very first stages of the reduction process, much before that Bi precipitates can be identified by AFM or optical microscopy, compared with Fig. 2 where we

present samples after long reduction times. For the G2, G3a, S1a, S1b, and S1c samples the *S* parameters attain a maximum and then decrease to the level corresponding to the *nonreduced* bulk material. The depth of the high-*S* layer moves towards the inside of the material with rising reduction times (compare G2 with G2a and S1b with S1c curves in Figs. 3 and 4, respectively). The *S* curves show, also, that some minimum “threshold” annealing time is needed to start the reduction process. We know from our previous research that long annealing times “saturate” the *S* parameter in bulk at high values (0.54 for Bi–Si glasses¹³). Differently from the *S* parameter, the *V* parameter falls monotonically with the implantation energy, it does not evolve in either type of glass and remains low (0.1 for the Ge glass and 0.16 for Si glass), indicating no nanovoids in the samples.

Therefore, we can use the dependence of the *S* parameter on energy in order to estimate the thickness of the reduced layer. Note that the exact determination of this thickness would require the knowledge of the diffusion length for positrons. Qualitatively, assuming that the point where the *S* parameter is in the midpoint between the minimal and maximal values is a mean value of the reduced layer thickness, we obtained the following results: 30 nm for S1a, 230 nm for S1b, and about 800 nm for S1c sample. The values for the Bi_{0.53}Si_{0.47}O_{1.72} samples are complementary to the results of the measurements of the thickness of S2–S5 samples.

The thicknesses of the high-*S* layer in the G2 and G2a samples are about 250 and 1000 nm, respectively. Note that for germanium glasses longer annealing times are needed to obtain the same depth of the reduced layer (2 h for the G2 sample give a similar depth as 0.8 h for S1c). Furthermore, the thickness of the reduced layer is higher in Si-based glasses compared to Ge glasses; this observation is seen also on a macroscopic scale in Fig. 2.

We note, also, a somewhat different behavior of the G2a sample—as far as all the other samples (including G2) show a rise of the *S* parameter in the near-to-surface layer (below 10 μm), the *S* parameter in the G2a sample “comes back” to the nonreduced value. We wonder if it is related in some way to the phenomena that cause the fall in the surface conductivity observed between the G2 and G2a samples, see Fig. 1.

Finally, it has been shown in other measurements,⁹ how a combination of *W* and *S* parameters can give information of a number of types for annihilation sites. In detail, the *W* vs *S* graph is composed of straight lines, connecting different points with Cartesian coordinates (*W*_{*i*}, *S*_{*i*}) if *i* types of defects (or phases) are present. For our data, only one segment is seen in Fig. 5, indicating the presence of just two phases, in agreement with the above model of the two-layer structure. Furthermore, from overlapping of *W*–*S* lines for two types of glasses one could deduce that these are preferentially bismuth-related sites where positrons are trapped; however, confirmation of this conclusion would require another positron-annihilation technique, i.e., the Doppler-coincidence one.^{14,15}

VII. CONCLUSIONS

Bismuth nanoclusters embedded in glass matrices and the surface layer of bismuth grains have been obtained by

thermal treatment in hydrogen atmosphere of $\text{Bi}_{0.33}\text{Ge}_{0.67}\text{O}_{1.84}$ and $\text{Bi}_{0.57}\text{Si}_{0.43}\text{O}_{1.72}$ glass. The changes of the electrical conductivity with increasing reduction times indicate the slower dynamics of the reduction process in Ge glass compared to Si glasses. Positron annihilation, optical microscopy, and also DSC, XRD, and AFM,¹¹ investigations confirm the layered structure of these glasses. The inner layer is a composite of bismuth nanocrystals embedded in SiO_2 or GeO_2 matrices. In particular, positron annihilation studies allow us to trace the evolution of the reduced layer in the early stages of annealing.

PAS studies show, also, that in the subnet of $\text{Si}(\text{Ge})\text{O}_2$ many vacancy-like defects exist. They probably allow the migration of Bi neutral atoms and quite free penetration of ingoing hydrogen molecules and outgoing water vapor. Use of the PAS technique, and comparison with our previous measurements on other stoichiometries of Bi glasses,¹³ shows that the thickness and depths of the reduced and intermediate layers can be changed starting from submicron values, in a wide, quite-well controlled range.

- ¹K. Nassau, D. L. Chadwick, and A. E. Miller, *J. Non-Cryst. Solids* **93**, 115 (1987).
- ²C. Lie, *Opt. Commun.* **4**, 2 (1983).
- ³H. J. L. Trap, *Acta Electron.* **14**, 41 (1971).
- ⁴Z. Pan, D. O. Henderson, and S. H. Morgan, *J. Non-Cryst. Solids* **171**, 134 (1994).
- ⁵K. Trzebiatowski, A. Witkowska, and T. Klimczuk, *Opt. Appl.* **30**, 677 (2000).
- ⁶B. Kusz, K. Trzebiatowski, and J. R. Barczyński, *Solid State Ionics* **159**, 293 (2003).
- ⁷B. Kusz and K. Trzebiatowski, *J. Non-Cryst. Solids* **319**, 257 (2003).
- ⁸B. Kusz, *Solid State Commun.* **125**, 623 (2003).
- ⁹R. S. Brusa, G. P. Karwasz, N. Tiengo, A. Zecca, F. Corni, G. Ottaviani, and R. Tonini, *Phys. Rev. B* **61**, 10154 (2000).
- ¹⁰A. Zecca, M. Bettonte, J. Paridaens, G. P. Karwasz, and R. S. Brusa, *Meas. Sci. Technol.* **9**, 409 (1998).
- ¹¹B. Kusz, K. Trzebiatowski, M. Gazda, and L. Murawski, *J. Non-Cryst. Solids* (in press).
- ¹²P. Ashoka-Kumar, K. G. Lynn, and D. O. Welch, *J. Appl. Phys.* **76**, 4935 (1994).
- ¹³D. Pliszka, M. Gazda, B. Kusz, K. Trzebiatowski, G. P. Karwasz, W. Deng, R. S. Brusa, and A. Zecca, *Acta Phys. Pol.* **99**, 465 (2001).
- ¹⁴R. S. Brusa, W. Deng, G. P. Karwasz, A. Zecca, and D. Pliszka, *Appl. Phys. Lett.* **79**, 1492 (2001).
- ¹⁵U. Myler and P. J. Simpson, *Phys. Rev. B* **56**, 14303 (1997).